Water Resources Research

RESEARCH ARTICLE
10.1029/2019WR025050

Special Section:
Advancing process representation in hydrologic models: Integrating new concepts, knowledge, and data

Predicting Shallow Groundwater Tables for Sloping Highland Aquifers

Tilashwork C. Alemie[1,2,3], Seifu A. Tilahun[2], Boris F. Ochoa-Tocachi[1,4,5], Petra Schmitter[6], Wouter Buytaert[1,4,5], J-Yves Parlange[7], and Tammo S. Steenhuis[2,7]

[1]Department of Civil and Environmental Engineering, Imperial College London, London, UK, [2]Faculty of Civil and Water Resources Engineering, Bahir Dar Institute of Technology, Bahir Dar University, Bahir Dar, Ethiopia, [3]Amhara Regional Agricultural Research Institute, Bahir Dar, Ethiopia, [4]Grantham Institute—Climate Change and the Environment, Imperial College London, London, UK, [5]Regional Initiative for Hydrological Monitoring of Andean Ecosystems—iMHEA, Quito, Ecuador, [6]International Water Management Institute, Yangon, Myanmar, [7]Department of Biological and Environmental Engineering, Cornell University, Ithaca, NY, USA

Abstract While hydrological science has made great strides forward during the last 50 years with the advance of computing power and availability of satellite images, much is unknown about the sustainable development of water for irrigation, domestic use, and livestock consumption for millions of households in the developing world. Specifically, quantification of shallow underground water resources for irrigation in highland regions remains challenging. The objective is to better understand the hydrology of highland watersheds with sloping hillside aquifers. Therefore, we present a subsurface flow model for hillside aquifers with recharge that varied from day to day. Recharge to the aquifer was estimated by the Thornthwaite Mather procedure. A characteristic time was identified for travel time of water flowing from the upper part of the hillside to the river or well. Using the method of characteristics, we found that the height of shallow groundwater level can be predicted by determining the total recharge over the characteristic time divided by drainable porosity. We apply the model to farmer-dug wells in the Ethiopian highlands using observed rainfall, potential evaporation, and a fitted travel time. We find that the model performs well with maximum water table heights being determined by the soil surface and minimum heights by the presence or absence of volcanic dikes downhill. Our application shows that unless the water is ponded behind a natural or artificial barrier, hillslope aquifers are unable to provide a continuous source of water during the long, dry season. This clearly limits any irrigation development in the highlands from shallow sloping groundwater.

Plain Language Summary The population in the Ethiopian highlands, similar to other developing countries, is rapidly increasing. In order to have enough food during the year, most families grow their food crops during the rainy season. More food can be grown by irrigation during the dry season. We mathematically tested and observed data of eight wells as to whether shallow aquifers on the sloping lands can store sufficient water during the rainy season so it can be used for irrigation after the rains have stopped. We found that groundwater on sloping soils is only available during the whole year when volcanic-derived subsurface barriers prevent flow downslope.

Key Points:
- A novel parsimonious model was developed for shallow hillslope groundwater tables
- Shallow groundwater depth in wells can be predicted from the recharge and the drainable porosity
- Hillslope aquifers cannot supply water for irrigation at end of the dry monsoon phase unless a downhill obstruction to flow is present

Supporting Information:
- Supporting Information S1
- Table S1

Correspondence to:
T. S. Steenhuis,
tss1@cornell.edu

Citation:
Alemie, T. C., Tilahun, S. A., Ochoa-Tocachi, B. F., Schmitter, P., Buytaert, W., Parlange, J.-Y., & Steenhuis, T. S. (2019). Predicting shallow groundwater tables for sloping highland aquifers. *Water Resources Research*, *55*, 11,088–11,100. https://doi.org/10.1029/2019WR025050

Received 24 FEB 2019
Accepted 22 NOV 2019
Accepted article online 11 DEC 2019
Published online 23 DEC 2019

1. Introduction

Leonardo da Vinci claimed five centuries ago that more was known about the celestial bodies than soils underfoot while little was known about water that was the driving force of all nature (Pfister et al., 2009). In many ways, that is still true today. Despite recent advances in large-scale groundwater assessments (e.g. Frappart & Ramillien, 2018, Tapley et al., 2004), the sustainable exploitation of local-scale phreatic underground water resources (i.e., sloping aquifers) in terrains other than plains and deltas is still understudied. These aquifers are becoming increasingly important in developing countries because the population has grown rapidly leading to deforestation, smaller landholdings, and food shortages. One of the ways to increase production is to increase the irrigation from aquifers during the dry phase and thereby provide a way to escape the poverty trap (Burney et al., 2013; Haider et al., 2018).

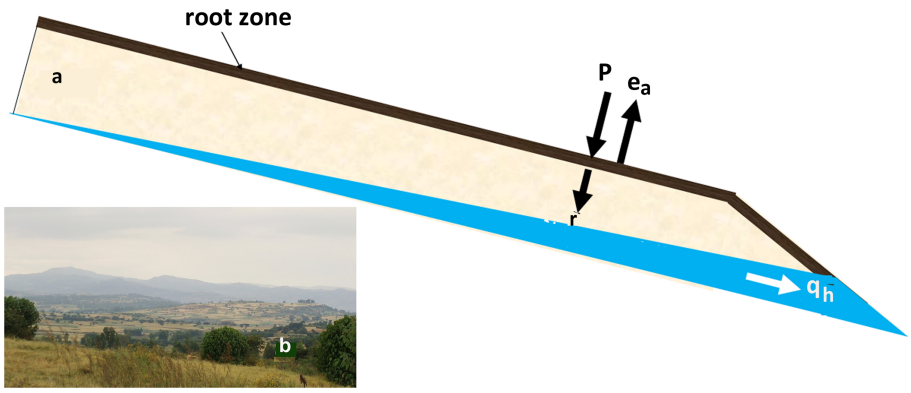

Figure 1. Shallow hillslope aquifer: (a) schematic diagram of a hillslope with fluxes considered in the water balance for soil profiles with shallow sloping aquifers; e_a is the actual evaporation; p is precipitation; r is recharge; and q_h is the interflow in the hillslope aquifer. Note that this is not drawn to scale. In reality, the slope is decreasing at the downhill side. (b) Actual hillslope in Ethiopian highlands in the Debre Mawi watershed.

The lack of properly calibrated analytical solutions and models for hillslope aquifer makes it difficult to realize the potential of these aquifers for small-scale irrigation. The hydraulic theory of sloping hillslope aquifers started with the formulations of Boussinesq (1877). Since then, many analytical and numerical solutions of the Boussinesq equation have been found (Bansal, 2016; Beven, 1981; Brutsaert, 1994; Parlange et al., 1981, 2000; Sanford et al., 1993; Stagnitti et al., 2004; Steenhuis et al., 1999). These analytical solutions to Boussinesq's equation are very useful to understanding the dynamics of subsurface flow processes along a hillslope (Troch et al., 2002). Only a few implementations (e.g., Kraijenhoff van de Leur, 1958) have considered the effect of a variable recharge pattern. Hillslope response to rainfall remains one of the central problems of catchment hydrology (Troch et al., 2003). Dralle et al. (2014) derived and used a new analytical technique to solve the hillslope Boussinesq's equation that analyzed the impact of the heterogeneity in recharge on water table dynamics and hillslope discharge prediction. Their results indicated that spatial distribution of recharge from a rainstorm is hydrologically significant on long, steep hillslopes. On short and small slopes, outflow patterns are only marginally affected by recharge distribution.

Most of the theories for hillslope aquifers involve predicting base and interflow at the base of the hillslope. Very few theories have been tested for predicting groundwater table levels on hillslopes (Rupp et al., 2004, 2009; Troch et al., 2013). The limitation of using only outflow data became apparent when subsurface flow models of varying complexity (Basha & Maalouf, 2005; Boll et al., 2015; Sloan & Moore, 1984; Steenhuis et al., 1999; Walker et al., 2015) fit equally well the outflow of the Coweeta hillslope published by Hewlett and Hibbert (1963). For an assessment of sustainable usage of groundwater supply for drinking and irrigation supply, accurate temporal water table heights matter. Therefore, models should be tested for whether they accurately can predict groundwater tables throughout the catchment.

Since irrigation is one of a few ways to escape the poverty trap in developing countries, this paper examines whether it is possible to store the water from the rain phase in the perched hillslope aquifer so that it can be used in the long dry phase. The objective of this paper is therefore to develop a parsimonious model to predict the spatial and temporal groundwater table heights for hand-dug wells located on hillslopes. We tested the model for the semihumid northwestern Ethiopian highlands in the Debre Mawi watershed with a distinct wet and dry period and variable recharge.

2. Theory

The theory is developed for unconfined shallow hillside aquifers in the tropical highlands with annual rainfall over 1,000 mm/year. These highlands have a monsoon climate with 4 months of rain and the remainder 8 months being mostly dry. The lands that are used for agriculture on the Ethiopian highlands hillsides are moderately sloping in the range of 3° to 16° (Akale et al., 2018) over distances of several hundred meters to kilometers (Figure 1b). The valley bottoms, with slopes from 1% to 3%, become saturated during the rain phase. Soils in the Ethiopian highlands are volcanic, which generally have a high matrix conductivity

(Jimenez et al., 2006) that is enhanced by self-organization of subsurface flow through macropores and through subsurface erosion (Mendoza & Steenhuis, 2002; Nieber & Sidle, 2010; Wilson et al., 2017). This can result in pipes that have been observed frequently in the Ethiopian highlands. Due to high conductivity of the volcanic soils, infiltration rates tend to be greater than the rainfall intensity in the Ethiopian highlands (Bayabil et al., 2010; Guzman, Tilahun, Dagnew, Zegeye, et al., 2017, Tilahun et al., 2015) and elsewhere (Buytaert et al., 2005). Water tables are up to 15 m deep.

When surface runoff by infiltration excess can be neglected, the mass balance for a hillslope aquifer can be written as (Figure 1a)

$$\frac{\partial S}{\partial t} = p - e_a - q_u \tag{1}$$

where $S$is the storage of water per unit area of hillside above the bedrock (L), p is the precipitation rate (L/T), e_a is the actual evaporation rate (L/T), and q_u is the base/interflow at the outlet averaged over the hillslope aquifer (L/T). When the soil is sufficiently deep, separate mass balances can be written for the root zone and the perched groundwater table.

2.1. Mass Balance for the Root Zone

The water balance for the storage, W,in root zone (L) is

$$\frac{\mathrm{d}W}{\mathrm{d}t} = p - e_a - r \tag{2}$$

where r is the percolation from the root zone (L/T).

The actual evaporation, e_a, and the percolation, r, can be calculated with the Thornthwaite Mather procedure (Thornthwaite & Mather, 1955; Steenhuis & Van der Molen, 1986). This method assumes that the actual evaporation decreases linearly with the available water in the soils (Lyra et al., 2016) from potential rate at field capacity to 0 at wilting point. Any water above field capacity percolates out of the root zone. Note that we follow here the convention in the equations that the rates are given in lower case. The daily values are given with capital letters and can be obtained by integrating the rates over the day. Formally, the Thornthwaite Mather procedure can be written for a daily time step as

$$P[t] \geq E_p[t] \qquad E_a[t] = E_p[t] \tag{3a}$$

$$P[t] < E_p[t] \qquad E_a[t] = P[t] + \frac{W[t-\Delta t]}{\Delta t}\left(1 - \exp\left(\frac{(P[t]-E_p[t])}{W_{fc}}\right)\right) \tag{3b}$$

where $P[t]$ is the precipitation (L/T) on day t (T), $E_p[t]$is the potential evaporation (L/T) on day t, $E_a[t]$ is the actual evaporation on day t, $W[t-\Delta t]$ is the available water in the root zone (L) on the previous day, and W_{fc} is the amount of water in root zone between field capacity and wilting point (L). The square brackets indicate the independent variable. The potential evaporation, E_p, was estimated using the Penman-Monteith method (Allen et al., 1998).

The available soil moisture content in the root zone, $W[t]$, is either equal to the maximum amount of water that can be stored at field capacity above wilting point in the root zone, W_{fc}, when the sum of rain and the previous moisture content is greater than field capacity, or otherwise it is simply the sum of the fluxes and the previous day's moisture content. Formally this can be written as

$$W[t] = \min\big((W[t-\Delta t] + (P[t]-E_a[t])\Delta t), W_{fc}\big) \tag{4a}$$

The excess above field capacity becomes the recharge, that is,

$$R[t] = \max\big(\big(W[t-\Delta t] + (P[t]-E_a[t])\Delta t - W_{fc}\big), 0\big) \tag{4b}$$

where $R[t]$ is the excess rain water that percolates daily downward on day t and $W[t]$ is related to the moisture content as $W[t] = d(\theta - \theta_{wp})$ where θ is the average moisture content of the root zone, θ_{wp} is the moisture content at wilting point, and d is the rooting depth.

2.2. Mass Balance for Hillslope Aquifer

The mass balance per unit area for a hillslope aquifer with a height h and infinite width can be written as

$$\mu \frac{\partial h}{\partial t} = -\frac{\partial q_h}{\partial x} + r \tag{5}$$

where h is the height of the water table above the bedrock (L), t is the time, x is length coordinate along the hillside with the origin at the groundwater divide (L), μ is the drainable porosity (L^3/L^3), q_h is the flow in the aquifer per unit width (L^2/T), and r is the recharge rate as a function of time (L/T). Inherently, it is assumed that in the mass balance in equation (5), the capillary effects can be neglected (Döll & Fiedler, 2008; Kong et al., 2013; Pauwels et al., 2002).

The lateral flux per unit width, q_h, in the aquifer according the Boussinesq's (1877) equation is

$$q_h = h\, K_s \sin\alpha - h\, K_s \cos\alpha \frac{\partial h}{\partial x} \tag{6}$$

where K_s is the saturated hydraulic conductivity and α is the angle of the bedrock. For convenience, the slope of the bedrock is often equated with the slope of the hill.

Combining equations (5) and (6) gives

$$\mu \frac{\partial h}{\partial t} = -\frac{\partial}{\partial x}(h\, K_s \sin\alpha) + \frac{\partial}{\partial x}\left(h\, K_s \cos\alpha\, \frac{\partial h}{\partial x}\right) + r \tag{7}$$

Solutions to equation (7) can be found in the literature for a variety of initial and boundary conditions. In all cases, the uphill boundary is the groundwater divide with a no-flow condition. For the downhill boundary at time, $t = 0$, the water table is dropped over some distance. Lastly, the initial condition consists of a water table of uniform height above the bedrock (i.e., a rectangle). The numerous analytical solutions to this problem are summarized in Rupp and Selker (2006). The rectangular initial form of the water table is not very realistic according to Van de Giesen et al. (2005). A water table configuration other than the rectangular shape for a hillslope aquifer is given by Steenhuis et al. (1999). They assume as a consequence of a constant rainfall rate an initial water table that is a triangular shape with zero height at the groundwater divide to a defined constant height at the outlet. The drainage from the hillside is predicted after the steady state rain stops and evaporation is prevented. For these conditions Steenhuis et al. (1999) show that not including the diffusivity term will violate the water table condition only close to the outlet for long times. The diffusivity term has little effect at short times and for most of the hillslope at longer times. This is consistent with other findings (Beven, 1981; Daly & Porporato, 2004; Dralle et al., 2014) that for long hillslopes with both relatively high conductivity and slope, the convective term dominates the diffusivity term.

The water table configuration for hillside aquifers in the highlands (Figure 1) is similar to those in Steenhuis et al. (1999) with one difference. The height of the water table at the downslope boundary is not constant but varies with the flux. The aquifer reaches the surface when the profile cannot transmit the subsurface discharge from the area above and some of the subsurface flow then becomes surface runoff. As a result, the saturated area expands for wetter conditions and contracts during dry periods. Although the exact shape of the water table is not investigated here, it is obvious that the second-order term in equation (7) becomes even less significant in determining the height of the water table.

Without the second-order term, equation (7) can be written as

$$\mu \frac{\partial h}{\partial t} = -\frac{\partial}{\partial x}(h\, K_s \sin\alpha) + r \tag{8}$$

This is the form of the equation used by Henderson and Wooding (1964) and employed by Beven (1981) in his kinematic wave model, tested by Sloan and Moore (1984) against the outflow of the Coweeta hillslope experiment, applied by Daly and Porporato (2004) for finding a solution of a recharge mound on a hillslope, and used by Steenhuis et al. (1988) in deriving a simple hillside model. Equation (8) has also been used to calculate the groundwater flow in models such as TOP model (Beven & Kirkby, 1979), THALES (Grayson et al., 1992), Soil Water Assessment Tool (Steenhuis et al., 2019) and the Parameter Efficient Distributed model (Tilahun et al., 2013).

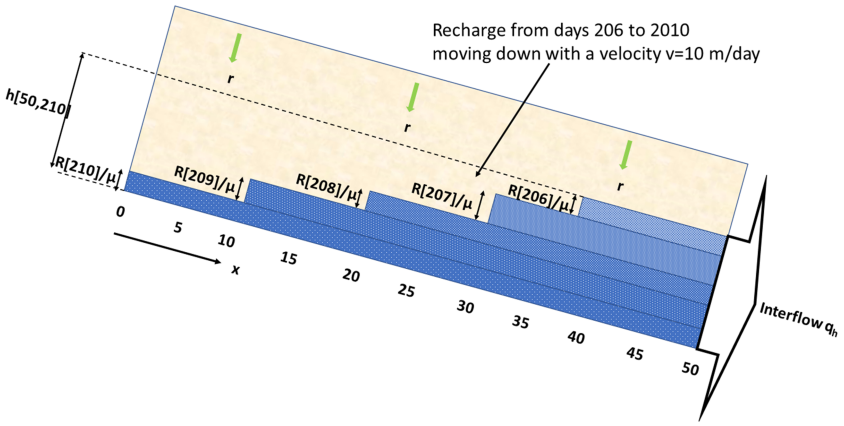

Figure 2. Illustration of water table height just after the water table was recharged on Day 210 for the upper 50 m of the soil profile. The velocity of the drying front is 10 m/day. Travel time from the top to the bottom of the slope is 5 days; each bar represents a daily recharge event $R[t]$; the height at the bottom of the hill, 50 m from the top on Day 210, is $h[x = 50, t = 210]$.

Equation (8) can be solved for the hillslope aquifer water table with the method of characteristics. This method avoids the problem with the point of stagnation at the top of the aquifer as identified by Stagnitti et al. (2004). Using this method, the water table height, $h[x,t]$, as a function of x along the hillside and time, can be written in integral form as (details are given in section A1)

$$h[x,t] = \frac{1}{\mu}\int_{t-\frac{x}{v}}^{t} r[\bar{t}]\,\mathrm{d}\bar{t} \qquad \text{for} \quad t \geq 0 \tag{9}$$

with the velocity of the drying front, v, expressed as

$$v = \frac{K_s \sin\alpha}{\mu} \tag{10}$$

and $r[t] = 0$ when $t < 0$. Note that in equation (9) $\frac{x}{v}$ is the travel time t_x from the groundwater divide to a point x downhill

$$t_x = \frac{x}{v} \tag{11}$$

Thus, equation (9) shows that after a pulse, if water is added, a drying front develops that starts at the groundwater divide (supporting information Figure S1) and moves downhill with a velocity, v. Since capillary effects are ignored, the moisture content just above the water table and behind the drying front is $(\theta_s - \mu)$ where θ_s is the saturated moisture content. Note that the conductivity in the "drained soil" is negligible and therefore water in the unsaturated soil is stationary with regard to lateral flow (Figure S1).

2.2.1. Multiple Recharge Events

Only daily rainfall records are available in developing countries. Using the Thornthwaite Mather procedure, daily recharge, R_i, values are calculated. Thus, $r[t]$ in equation (9) is a discrete set of recharge amounts, and the integral is replaced by summation. Hence, we find that for daily recharge values with daily time steps, the water table height in equation (9) on Day t at x can be written as (Figure 2)

$$h[x,t] = \frac{1}{\mu} \sum_{i=t-t_x}^{i=t} R_i \tag{12}$$

where t is the day that the water table height at x is calculated and t_x is the travel time of the drying front in days from the divide to x. Both t and t_x are expressed in days and therefore are integer values. Each day has a recharge amount, R_i. The rounding off to days is warranted because the exact time of rainfall that the

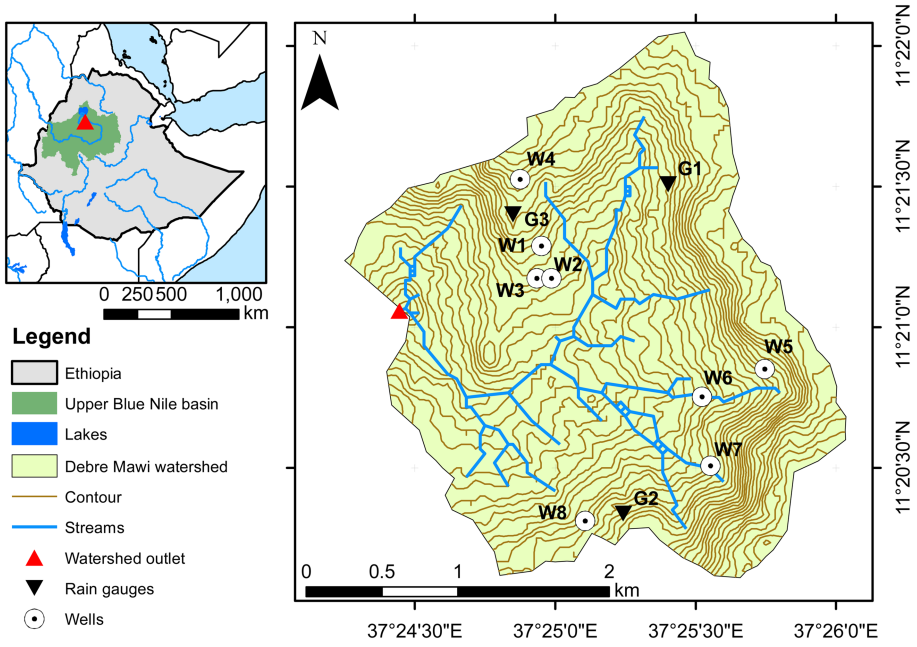

Figure 3. Location of hand-dug wells monitored during the rainy season in 2016 and the dry season in 2017 in the Debre Mawi watershed (W1–W8 represent locations of wells) and location of rain gauges that were used for daily rainfall depth monitoring from May 2016 to December 2017 (G_1–G_3 represent locations of rain gauges).

recharge reaches the shallow groundwater is not known. When needed, the solution for partial days and noninteger travel times can be found with equation (9) rather easily.

Finally, the water table height has an upper and lower limit. The upper limit is the soil surface. The lower limit is determined by volcanic dikes, artificial subsurface barriers, or a static groundwater level in the well, $h_{\min}[x]$, to be added to the earlier predicted height. With these two additions, the height of the sloping aquifer calculated in equation (12) can be written as

$$h[x,t] = \min\left[\left(h_{\min}[x] + \sum_{i=t-t_x}^{t} \frac{R_i}{\mu}\right), D[x]\right] \tag{13}$$

where $D[x]$ is the height of the soil surface above the bedrock and at locations where wells are installed. $D[x]$ is equal to the depth of the well from the surface. Although not tested in the manuscript, we can show that flux per unit area is equal to the average recharge over t_x. The details are given in the section A2.

3. Materials and Methods

3.1. Description of the Watershed

The theory for the water table height was tested in the Debre Mawi watershed in the head waters of the Blue Nile in Ethiopia. The Debre Mawi watershed is situated about 30 km south of Lake Tana (between 11°20′13″ and 11°21′58″N and 37°24′07″ and 37°25′55″E). The watershed's total area is 716 ha, and the elevation ranges between 1,950 and 2,309 m. The watershed is characterized as mountainous, highly rugged and dissected topography with steep slopes (Guzman et al., 2013). Slopes vary from 8% to 30%. The maximum daytime temperature of 26°C occurs in March and April with the minimum temperature of 8°C in November and December (Dagnew et al., 2015). The watershed has a unimodal rainfall regime with an average annual rainfall of 1,238 mm/year (Zegeye et al., 2010). June, July, August, and September receive around 80% of the annual rainfall. Potential evapotranspiration is 2–3 mm/day in the rain phase and 4–5 mm/day during the dry phase. Seventy percent of the watershed area is cultivated land. The remaining area is brush on the steep lands and grasslands in the periodically saturated areas in valley bottoms and areas above volcanic dikes (Amare et al., 2014).

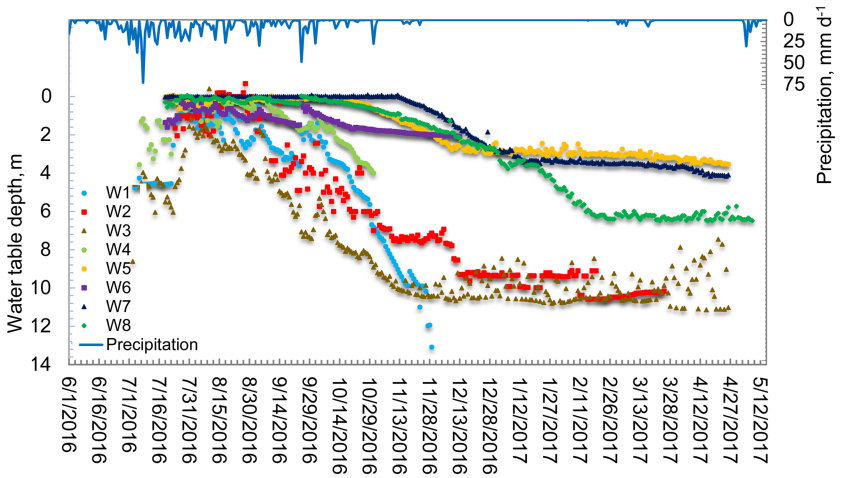

Figure 4. Precipitation and water table depth from the soil surfaces for the eight hand-dug wells in the Debre Mawi watershed in 2016 and 2017.

The watershed is underlain by shallow, highly weathered, and fractured basalt. The fractures are highly interconnected with limited clay infillings but at some locations are blocked by lava dikes. The main soil types in the watershed include vertic nitosols (locally known as *Silehana*) located at the major midslope positions. It is reddish brown and commonly used for growing tef. Nitosol soils (locally, *Dewel*) in the upper part of the watershed are deep, well-drained productive red clay loams. Finally, vertisols (locally, *Walka*) cover the major lower slope area in the watershed and are partially saturated during the middle and end of the rain phase.

In 2015, during the dry season, in order to counteract water scarcity, farmers, mainly on their own initiative, began installing hand-dug wells in locations with acacia trees with the intent to provide water for domestic use, irrigation of small plots of vegetables, and fattening calves for income generation.

3.2. Data Collection

3.2.1. Climatic Data

From May 2016 to December 2017, daily rainfall depth was recorded using one automatic tipping bucket rain gauge and three manually read rain gauges (Figure 3). The automatic rain gauge and one of the three manual rain gauges were installed at G_1, while the other two manual rain gauges were installed at G_2 and G_3 (Figure 3). Potential evaporation was calculated with the Penman-Monteith method using data collected at the National Meteorological station at Bahir Dar, located 30 km north of the watershed.

Table 1
Dimensions and Related Descriptions of Wells in the Debre Mawi Watershed

Well ID	Depth (cm)	Minimum water level (cm)	Monitoring period[a]	Remarks based on field observation
W1	1,570	262	7/6/2016 to 11/15/2016	Water table reduces rapidly after rain phase
W2	1,100	42	7/6/2016 to 3/25/2017	The site dominated by rocky outcrop soil
W3	1,170	41	7/6/2016 to 4/26/2017	Similar to W2, but the soil is less rocky
W4	1,050	450	7/6/2016 to 10/31/2016	Farmer stopped monitoring before the water level reached the bottom of the well
W5	500	148	7/19/2016 to 7/26/2017	Perennial well although water amount is minimal during dry season
W6	233	25	7/19/2016 to 12/13/2016	Perennial, potentially good water supply. Acacia trees nearby. Depth reduced from 11 to 2.3 m due to caving in of well
W7	920	500	7/19/2016 to 4/26/2017	Perennial, protected well with acacia trees in its immediate proximity
W8	710	62	7/19/2016 to 5/8/2017	Perennial, site looks rocky, and has green grass during dry season. Site is close to acacia trees

[a]Dates are formatted as month/date/year.

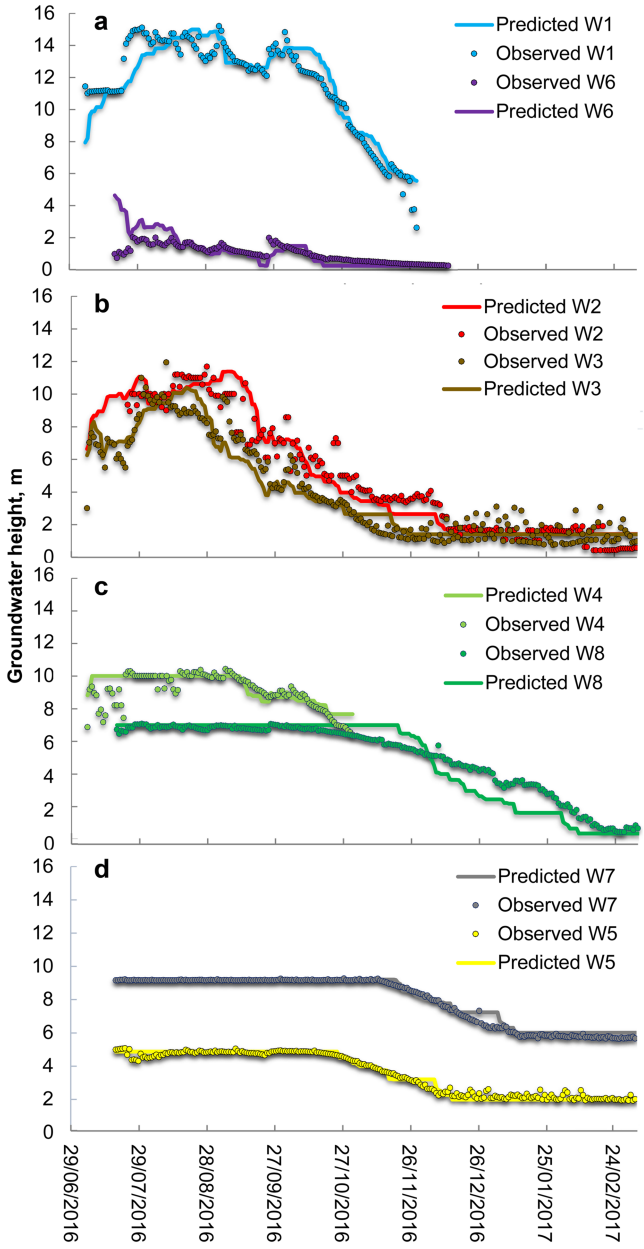

Figure 5. Observed and predicted water table heights above the bedrock of the eight monitored wells in the Debre Mawi watershed: (a) Wells W1 and W6; (b) Wells W2 and W3; (c) Wells W4 and W8; (d) Wells W5 and W7.

3.2.2. Groundwater Table Measurements

Groundwater table heights were measured in eight hand-dug wells distributed over the catchment (Figures 3 and 4). From July 2016 to May 2017, daily water table heights of wells were determined by averaging two measurements taken each morning (8:00 a.m.) and evening (6:00 p.m.). Water levels in wells were recorded by the farmers who own them. Measurements were stopped at the time the water levels became too low to fetch water. In two cases, monitoring was stopped prematurely: Well W6 collapsed, and the owner of W4 stopped monitoring (Table 1 and Figure 4).

3.3. Prediction of the Groundwater Level

The prediction of the water level is based on equation (14) where the recharge was calculated using the Thornthwaite Mather procedure. In addition, five physical parameters were needed: maximum available water in the root zone, W_{fc} (in equations (3) and (4)); drainable porosity, μ; minimum water level in the well, $h_{\min}$; the depth of the well, $D[x]$; and the maximum travel time, t_x. The values of W_{fc} and μ are considered uniform across the watershed. Based on initial calibration, a value of $\mu = 0.049$ was selected. This is smaller than the value of 0.20 assumed by Guzman, Tilahun, Dagnew, Zimale, et al. (2017) for the more porous surface soil in Debre Mawi. The maximum available water in the root zone was set to 30 mm based on Tilahun et al. (2013). The minimum water level, $h_{\min}$, and the well depth, $D[x]$, were measured for each well (Table 1). In cases where the water table intersects the surface (i.e., water is seeping out of the hillside), the water table was set equal to the surface. The flow of water in Wells W5 to W8 in the southeastern part of the watershed were blocked by volcanic dykes and were perennial. Thus, the only parameter that was fit for each well independently was the travel time, t_x. Finally, we fit a travel time.

4. Results and Discussion

In this section, we present first the observed water table depths. Subsequently, we predict the water level above the bedrock based on equation (13) using the recharge calculated with equations (3) and (4).

4.1. Observed Water Table Depths

All wells are located near acacia trees, and most have rocks at the surface (see Figure S3). The water table depths in the wells are shown in Figure 4. On 6 July 2016, water level measurements started for Wells W1–W4 in the northwestern part of the watershed (Figure 4). Water levels were still increasing at that time. On 19 July 2016, water level observations commenced for Wells W5–W8 in the southeast. The water levels for three of the wells (W5, W7, and W8) were within 50 cm of the soil surface at times and remained near the surface during the entire rain phase and first part of the dry phase (Figure 4). Well W6 was 2 m deep on 19 July and still rising. This well collapsed during the rain phase. The water levels in all the wells were at their highest at the end of July or the beginning of August. Water levels in wells W1, W2, and W3 were near the bottom around the end of 2016 (Figures 4 and 5). Observation of Well W4 ceased before the water level reached the bottom of the well. The observed water levels in Well W3 after December fluctuated by 3 m which might be due to taking water out for irrigation. Well W5 had only a limited supply during the dry phase, while W7 and W8 had abundant supplies. These two wells were in an area with volcanic outcrops.

Table 2
Summary of Hand-Dug Well Simulations

Well ID	Well depth (m)	Travel time t_x (days)	Regression coefficient (R^2)	Slope regression
W1	15.7	110	0.84	1.00
W2	11.0	75	0.94	1.00
W3	11.7	55	0.91	0.96
W4	10.5	47	0.29	1.02
W5	5.0	75	0.97	1.01
W6	2.3	16	0.46	1.17
W7	9.2	103	0.96	1.02
W8	7.1	130	0.94	1.00

Note. Travel time, t_x, values were obtained such that observed and predicted values agreed best. Regression coefficient and slope are obtained by regressing observed versus predicted values.

4.2. Predicted Water Table Depths

4.2.1. Simulating the Water Levels in Wells

The first step in predicting the water height is calculating the recharge to the groundwater with the Thornthwaite Mather procedure (equations (2) and (3) and Figure S2). The maximum water content available to the plant in the root zone was 30 mm. We assumed that the percolation would arrive at the water table on the same day and no water would be needed for wetting up the soil profile. As seen in Figure 5, this caused the model prediction to deviate from the observed values in the beginning of the simulation period.

4.2.2. Predicting Water Hheight Above Bedrock

The simulated water height in the wells above the bedrock are shown in Figure 5. The input data, the fitted travel time values, and well depth, together with the R^2, are given in Table 2. For four of the eight wells (W4, W5, W7, and W8), water table heights were restrained by the soil surface, while for the four remaining wells, water levels were not affected by the soil surface. For the four wells in the southeastern part of the watershed (W5 to W8), a minimum water level was needed. In general, a good fit was obtained with R^2 values over 80% for six of the eight wells (Table 2 and Figure 5). Although the trend was predicted correctly, two wells, W4 (poor data collection) and W6 (well collapsed) had a poor R^2.

In the beginning of the rain phase, water levels in three of the wells (W3, W4, and W6) were overestimated likely because the model assumed that all the water percolating from the root zone arrived at the groundwater as recharge. However, in the beginning of the rainy season, some of this water was used to wet the soil profile. Hence, the water levels were overestimated in the beginning. It is likely that this was the case in the other wells as well, but as measurements started sometime after the first rains and the water levels were already at the surface, effects of overprediction were minimal.

It is often assumed by hydrologists in watershed simulations that the groundwater and the watershed divide coincide. In this manuscript, the travel time from the divide was fitted and calculated. As demonstrated by W8, the divide did not coincide for the Debre Mawi watershed. The fitted travel time was 130 days (Table 2), while, as shown in Figure 3, Well W8 is located nearly on the surface watershed divide. It is very likely that the subsurface flow path follows the divide just south of the watershed boundary (Figure 3).

In the beginning of the rain phase, the model did not fit the well data satisfactorily because the linearization of the Boussinesq's equation introduced errors at that stage. After 300 or 400 mm of cumulative rainfall at the end of the dry season, most rainfall in excess of potential evaporation becomes recharge, and the recharge predictions become more robust (Liu et al., 2008; Ochoa-Tocachi et al., 2018). More detailed subsurface data would only partly aid in simulating the wet-up period accurately.

It is customary to compare the results with the findings in the literature. Hillslope models are mainly validated with discharge data. Recent testing shows that the daily interflow by our model is predicted well by averaging the recharge over the subsurface travel time as detailed in section A3. Comparison with model results are rare in the literature. Rupp et al. (2009) fitted a slightly more complex solution to the Boussinesq's equation to well data, and the fit was equally good for the solutions of Rupp and coworkers and presented here.

In summary, the hillslope model developed is simple: Water table height and recharge are determined by adding or averaging, respectively, the excess rainfall over a fixed period previous to the day of observation. More complex approaches based on the Richards' equation are available, but as Beven (1981), Grayson et al. (1992), and Mirus et al. (2011) all note, in actual landscapes, many of the advantages of the complex solutions are annulled by the ambiguity of the input parameter values, the complexity of the landscape, and the heterogeneity of subsurface flow parameters.

5. Conclusions

This paper developed a model for predicting groundwater table heights on hillsides to examine whether it is possible to store water from the rain phase in a perched hillslope aquifer so that it can be used in the dry phase

for irrigation to increase agricultural production. The groundwater table was predicted as the quotient of the sum of the recharge over the travel time from the divide to the well and the drainable porosity. A minimum of input data was needed consisting of the well characteristics, drainable porosity, precipitation, and potential evaporation. The predicted and the observed water table data fit well. The travel time of the groundwater was in the order of 3 to 4 months. This means that the wells will run out of water after this relatively short period unless volcanic dikes downstream keep the water at a minimum level. Finding the travel time might not be as simple for hydrologists as envisioned in section 2 since in the volcanic landscape, the surface and subsurface watershed boundaries do not coincide due to the presence of faults conducting water over long distances. Geological surveys are required to find travel times a priori.

Future research should examine closely the wetting of the watershed after the dry phase and its effect on the recharge to the water table. In addition, the theory should be tested in the future on its ability to predict both the stream discharge and the piezometer data from watersheds where both are available. Finally, the volcanic landscape is highly complex and variable, and therefore the relationship of the effective parameters and the underlying geological formations should be examined.

Appendix A: Solving for the Flux and Water Table Height for a Hillslope Aquifer Using Method of Characteristics

A.1. Finding Solutions With the Method of Characteristics for Any Rainfall Function

Consider the solution of equation (8) with the method of characteristics for a recharge rate, $r[t]$

$$\mu\frac{\partial h}{\partial t} = -K_s\sin\alpha\frac{\partial h}{\partial x} + r \tag{A1}$$

The initial condition is that $h = 0$ for all x at time $t = 0$ and the boundary condition is that $h = 0$ at $x = 0$ for all times.

Using the method of characteristics, equation (A1) can be written as

$$\frac{\mathrm{d}t}{\mu} = \frac{\mathrm{d}x}{K_s\sin\alpha} = \frac{\mathrm{d}h}{r} \tag{A2}$$

Integrating the first two terms gives

$$x = vt + x_0 \tag{A3}$$

where x_0 is an integration constant and

$$v = \frac{K_s\sin\alpha}{\mu} \tag{A4}$$

Integrating the first and last term in equation (A2) results in

$$h = \frac{\int_0^t r[\bar{t}]\mathrm{d}\bar{t}}{\mu} + h_0 \tag{A5}$$

where h_0 is an integration constant. To find the integration constant, we write h_0 as a function of x_0, or

$$\mu h = \int_0^t r[\bar{t}]\mathrm{d}\bar{t} + \mu h_0[x - vt] \tag{A6}$$

Using the initial condition for $t = 0$, $h = 0$ for all $x > 0$ in equation (A6) indicates that $h_0[x] = 0$. Thus, $h_0[x - vt]$ in equation (A6) must be 0 for $x - vt > 0$; that is,

$$h_0[x-vt] = 0 \qquad \text{if } x-vt>0 \tag{A7}$$

Using the boundary condition that when $x = 0$, $h = 0$, we can write equation (A6) as

$$\mu h_0[-vt] = -\int_0^t r[\bar{t}]\mathrm{d}\bar{t} \tag{A8}$$

Consequently, in equation (A8) for any $y < 0$,

$$\mu h_0[y] = -\int_0^{\frac{y}{v}} r[\bar{y}]\mathrm{d}\bar{y} \tag{A9}$$

If we take $y = x - vt$, equation (A9) can be written as

$$h_0[x-vt] = \frac{-\int_0^{\frac{-x-tv}{v}} r[\bar{t}]\mathrm{d}\bar{t}}{\mu} \qquad \text{if } x-vt<0, \tag{A10}$$

Substituting $h_0 = 0$ from equation (A7) in equation (A5) results in

$$h = \frac{\int_0^t r[\bar{t}]\mathrm{d}\bar{t}}{\mu} \qquad \text{if} \qquad x-vt>0, \tag{A11}$$

and using equation (A10) in equation (A5) gives

$$h[x,t] = \frac{1}{\mu}\left(\int_0^t r[\bar{t}]\mathrm{d}\bar{t} - \left(H\left[t-\frac{x}{v}\right]\right)\int_0^{t-\frac{x}{v}} r[\bar{t}]\mathrm{d}\bar{t}\right) \tag{A12}$$

where the Heavyside function, H, is defined as $H\left[t-\frac{x}{v}\right] = 0$ when $\left(t-\frac{x}{v}\right)<0$ and $H\left[t-\frac{x}{v}\right] = 1$ when $\left(t-\frac{x}{v}\right)>0$ Equation (A12) can be written in a compact form as

$$h[x,t] = \frac{1}{\mu}\int_{t-\frac{x}{v}}^t r[\bar{t}]\mathrm{d}\bar{t} \tag{A13}$$

where $r[\bar{t}] = 0$ when $\bar{t}<0$.

Note that in equation (A13), $\frac{x}{v}$ is the travel time, t_x, from the groundwater divide to a point, x, downhill. Thus, equation (A13) shows that the water table height at a point, x, and time, t, can be found by the total rainfall in the prior t_x days divided by the drainable porosity where t_x is the travel time of drying front from the divide to x (as indicated above).

A.2. Equations for Interflow on a Hillslope

The flux per unit width, $q_h[x,t]$, at x and time, t, can be obtained as follows

$$q_h[x,t] = vh\mu \tag{A14}$$

Then by employing equations (A13) and (A15)

$$q_h[x,t] = v\int_{t-\frac{x}{v}}^t r[\bar{t}]\mathrm{d}\bar{t} \tag{A15}$$

Substituting $v = \frac{x}{t_x}$ in equation (A16), we find that

$$q_h[x,t] = x\int_{t-t_x}^t \frac{r[\bar{t}]\mathrm{d}\bar{t}}{t_x} \tag{A17}$$

The flux per unit width at x is, thus, equal to the average recharge over the travel time from the divide to x (e.g., $\int_{t-t_x}^t \frac{r[\bar{t}]}{t_x}\mathrm{d}\bar{t}$) multiplied by the distance to the divide.

Rewriting equation (A17) for daily values of the recharge, R_i

$$q_h[x,t] = x \sum_{i=t-t_x}^{i=t} \frac{R_i}{t_x} \quad \text{(A18)}$$

Acknowledgments
This research was funded mainly by the UK Research Council NERC/ESRC/DFID ESPA programme (Project NE-K010239-1, "Adaptive governance of mountain ecosystem services for poverty alleviation enabled by environmental virtual observatories"). Partial support was received by the Innovation Laboratory for Small Scale Irrigation (ILSSI) project (AID-OAA-A-13-000SS) funded by Feed the Future through the U.S. Agency for International Development and by the CGIAR Research Program on Water, Land and Ecosystems (WLE) with funded by the CGIAR Trust Fund donors. The contents of the manuscript do not necessarily reflect the views of USAID, the United States Government, and the UK Research Council. The data on which this manuscript is based are included as Table S1 in the supporting information.

References

Akale, A. T., Moges, M. A., Dagnew, D. C., Tilahun, S. A., & Steenhuis, T. S. (2018). Assessment of nitrate in wells and springs in the north central Ethiopian highlands. *Water*, *10*, 476. https://doi.org/10.3390/w10040476

Allen, R. G., Pereira, L. S., Raes, D., & Smith, M. (1998). FAO irrigation and drainage paper no. 56. Crop evapotranspiration (guidelines for computing crop water requirements). *Technical Report 56, Food and Agriculture Organization*, Rome, Italy

Amare, T., Zegeye, A. D., Yitaferu, B., Steenhuis, T. S., Hurni, H., & Zeleke, G. (2014). *Ecohydrology & Hydrobiology*, *14*, 192–199. https://doi.org/10.1016/j.ecohyd.2014.07.002

Bansal, R. K. (2016). Approximate analytical solution of Boussinesq equation in homogeneous medium with leaky base. *Applications and Applied Mathematics: An International Journal (AAM)*, *11*(1), 184–191. http://pvamu.edu/aam

Basha, H. A., & Maalouf, S. F. (2005). Theoretical and conceptual models of subsurface hillslope flows. *Water Resources Research*, *41*, W07018. https://doi.org/10.1029/2004WR003769

Bayabil, H. K., Tilahun, S. A., Collick, A. S., Yitaferu, B., & Steenhuis, T. S. (2010). Are runoff processes ecologically or topographically driven in the (sub) humid Ethiopian highlands? The case of the Maybar watershed. *Ecohydrology*, *3*, 457–466. https://doi.org/10.1002/eco.170

Beven, K. (1981). Kinematic sSubsurface stormflow. *Water Resources Research*, *17*(5), 1419–1424. https://doi.org/10.1029/WR017i005p01419

Beven, K. J., & Kirkby, M. J. (1979). A physically based variable contributing area model of basin hydrology. *Hydrological Sciences Bulletin*, *24*, 43–69. https://doi.org/10.1080/02626667909491834

Boll, J., Brooks, E. S., Crabtree, B., Dun, S., & Steenhuis, T. S. (2015). Variable source area hydrology modeling with the water erosion prediction project model. *JAWRA Journal of the American Water Resources Association*, *51*(2). https://doi.org/10.1111/1752-1688.12294

Boussinesq, J. (1877). Essai sur la theorie des eaux courantes. *Memoires presentes par divers savants a l'Academie des Sciences de l'Institut National de France*, *23*(1), 252–260.

Brutsaert, W. (1994). The unit response of groundwater outflow from a hillslope. *Water Resources Research*, *30*(10), 2759–2763. https://doi.org/10.1029/94WR01396

Burney, J. A., Naylor, R. L., & Postel, S. L. (2013). The case for distributed irrigation as a development priority in sub-Saharan Africa. *PNAS*, *110*(31), 12513–12517. https://doi.org/10.1073/pnas.1203597110

Buytaert, W., Wyseure, G., De Bièvre, B., & Deckers, J. (2005). The effect of land-use changes on the hydrological behaviour of Histic Andosols in south Ecuador. *Hydrological Processes*, *19*, 3985–3997. https://doi.org/10.1002/hyp.5867

Dagnew, C. D., Guzman, C. D., Zegeye, A. D., Tebebu, T. Y., Getaneh, M., Abate, S., et al. (2015). Impact of conservation practices on runoff and soil loss in the sub–humid Ethiopian highlands: The Debre Mawi watershed. *Journal of Hydrology and Hydromechanics*, *63*(3), 210–219. https://doi.org/10.1515/johh-2015-0021

Daly, E., & Porporato, A. (2004). A note on groundwater flow along a hillslope. *Water Resources Research*, *40*, W01601. https://doi.org/10.1029/2003WR002438

Döll, P., & Fiedler, K. (2008). Global-scale modeling of groundwater recharge. *Hydrology and Earth System Sciences*, *12*, 863–885. https://doi.org/10.5194/hess-12-863-2008

Dralle, D. N., Boisramé, G. F. S., & Thompson, S. E. (2014). Spatially variable water table recharge and the hillslope hydrologic response: Analytical solutions to the linearized hillslope Boussinesq equation. *Water Resources Research*, *50*, 8515–8530. https://doi.org/10.1002/2013WR015144

Frappart, F., & Ramillien, G. (2018). Monitoring groundwater storage changes using the gravity recovery and climate experiment (GRACE) satellite mission*: A Review. Remote Sensing*, *10*, 829. https://doi.org/10.3390/rs10060829

Grayson, R. B., Moore, I. D., & McMahon, T. A. (1992). Physically based hydrologic modeling, 1, A terrain-based model for investigative purposes. *Water Resources Research*, *28*, 2639–2658. https://doi.org/10.1029/92WR01258

Guzman, C. D., Tilahun, S. A., Dagnew, D. C., Zegeye, A. D., Tebebu, T. Y., Yitaferu, B., & Steenhuis, T. S. (2017). Modeling sediment concentration and discharge variations in a small Ethiopian watershed with contributions from an unpaved road. *Journal of Hydrology and Hydromechanics*, *65*(1), 1–17. https://doi.org/10.1515/johh-2016-0051

Guzman, C. D., Tilahun, S. A., Dagnew, D. C., Zimale, F. A., Zegeye, A. D., Boll, J., et al. (2017). Spatio-temporal patterns of groundwater depths and soil nutrients in a small watershed in the Ethiopian highlands: Topographic and land-use controls. *Journal of Hydrology*, *555*, 420–434. https://doi.org/10.1016/j.jhydrol.2017.09.060

Guzman, C. D., Tilahun, S. A., Zegeye, A. D., & Steenhuis, T. S. (2013). Suspended sediment concentration–discharge relationships in the (sub) humid Ethiopian highlands. *Hydrology and Earth System Sciences*, *17*, 1067–1077. https://doi.org/10.5194/hess-17-1067-2013

Haider, L. J., Boonstra, W. J., Peterson, G. D., & Schlüter, M. (2018). Traps and sustainable development in rural areas: A review. *World Development*, *101*, 311–321. https://doi.org/10.1016/j.worlddev.2017.05.038

Henderson, F. M., & Wooding, R. A. (1964). Overland flow and groundwater flow from a steady rainfall of finite duration. *Journal of Geophysical Research*, *69*(8), 1531–1540. https://doi.org/10.1029/JZ069i008p01531

Hewlett, J. D., & Hibbert, A. R. (1963). Moisture and energy conditions within a sloping soil mass during drainage. *Journal of Geophysical Research*, *68*(4), 1081–1087. https://doi.org/10.1029/JZ068i004p01081

Jimenez, C. C., Tejedor, M., Morillas, G., & Neris, J. (2006). Infiltration rate in Andisols: Effect of changes in vegetation cover (Tenerife, Spain). *Journal of Soil and Water Conservation*, *61*, 153–158.

Kong, J., Shen, C.-J., Xin, P., Song, Z., Li, L., Barry, D. A., et al. (2013). Capillary effect on water table fluctuations in unconfined aquifers. *Water Resources Research*, *49*, 3064–3069. https://doi.org/10.1002/wrcr.20237

Kraijenhoff van de Leur, D. A. (1958). A study of non-steady groundwater flow with special reference to a reservoir coefficient. *De Ingenieur 70. Bouw- en Waterkunde*, *9*, B87–B94.

Liu, B. M., Collick, A. S., Zeleke, G., Adgo, E., Easton, Z. M., & Steenhuis, T. S. (2008). Rainfall-discharge relationships for a monsoonal climate in the Ethiopian highlands. *Hydrological Processes*, *22*, 1059–1067. https://doi.org/10.1002/hyp.7022

Lyra, G. B., de Souza, L. L., da Silva, E. C., Lyra, G. B., Teodoro, I., Ferreira-Júniord, R. A., & Renan de Souza, R. C. (2016). Soil water stress co-efficient for estimating actual evapotranspiration of maize in north-eastern Brazil. *Meteorological Applications*, *23*, 26–34. https://doi.org/10.1002/met.1516

Mendoza, G., & Steenhuis, T. S. (2002). Determination of hydraulic behavior of hillsides with and hillslope infiltrometer. *Soil Science Society of America Journal*, *66*, 1501–1504. https://doi.org/10.2136/sssaj2002.1501

Mirus, B. B., Ebel, B. A., Heppner, C. S., & Loague, K. (2011). Assessing the detail needed to capture rainfall runoff dynamics with physics based hydrologic response simulation. *Water Resources Research*, *47*, W00H10. https://doi.org/10.1029/2010WR009906

Nieber, J. L., & Sidle, R. C. (2010). How do disconnected macropores in sloping soils facilitate preferential flow? *Hydrological Processes*, *24*, 1582–1594. https://doi.org/10.1002/hyp.11212

Ochoa-Tocachi, B. F., Alemie, C. T., Guzman, C. D., Tilahun, S. A., Zimale, F. A., Buytaert, W., & Steenhuis, T. S. (2018). Sensitivity analysis of the Parameter-Efficient Distributed (PED) model for discharge and sediment concentration estimation in degraded Humid landscapes. *Land Degradation and Development*. https://doi.org/10.1002/ldr.3202

Parlange, J.-Y., Braddock, R. D., & Sander, G. C. (1981). Analytical approximations to the solution of the Blasius equation. *Acta Mechanica*, *38*(1-2), 119–125. https://doi.org/10.1007/BF01351467

Parlange, J.-Y., Hogarth, W. L., Govindaraju, R. S., Parlange, M. B., & Lockington, D. (2000). On an exact analytical solution of the Boussinesq equation. *Transport in Porous Media*, *39*, 339–345. https://doi.org/10.1023/A:1006504527622

Pauwels, V. R. N., Verhoest, N. E. C., & Troch, F. P. D. (2002). A metahillslope model based on an analytical solution to a linearized Boussinesq equation for temporally variable recharge rates. *Water Resources Research*, *38*(12), 1297. https://doi.org/10.1029/2001WR000714

Pfister, L., Savenije, H. H. G., & Fenicia, F. (2009). Leonardo Da Vinci's water theory: On the origin and fate of water. IAHS Special Publications 9

Rupp, D. E., Owens, J. M., Warren, K. L., & Selker, J. S. (2004). Analytical methods for estimating saturated hydraulic conductivity in a tile-drained field. *Journal of Hydrology*, *289*(1-4), 111–127.

Rupp, D. E., Schmidt, J., Woods, R. A., & Bidwell, V. J. (2009). Analytical assessment and parameter estimation of a low-dimensional groundwater model. *Journal of Hydrology*, *377*, 143–154. https://doi.org/10.1016/j.jhydrol.2009.08.018

Rupp, D. E., & Selker, J. S. (2006). On the use of the Boussinesq equation for interpreting recession hydrographs from sloping aquifers. *Water Resources Research*, *42*, W12421. https://doi.org/10.1029/2006WR005080

Sanford, W. E., Parlange, J.-Y., & Steenhuis, T. S. (1993). Hillslope drainage with sudden drawdown: Closed form solution and laboratory experiments. *Water Resources Research*, *29*(7), 2313–2321. https://doi.org/10.1029/93WR00515

Sloan, P. G., & Moore, I. D. (1984). Modelling subsurface stormflow on steeply sloping forested watersheds. *Water Resources Research*, *20*(12), 1815–1822. https://doi.org/10.1029/WR020i012p01815

Stagnitti, F., Li, L., Parlange, J.-Y., Brutsaert, W., Lockington, D. A., Steenhuis, T. S., et al. (2004). Drying front in a sloping aquifer: Nonlinear effects. *Water Resources Research*, *40*, W04601. https://doi.org/10.1029/2003WR002255

Steenhuis, T. S., Parlange, J.-Y., Sanford, W. E., Heilig, A., Stagnitti, F., & Walter, M. F. (1999). Can we distinguish Richards' and Boussinesq's equations for hillslopes? The Coweeta experiment revisited. *Water Resources Research*, *35*(2), 589–593. https://doi.org/10.1029/1998WR900067

Steenhuis, T. S., Schneiderman, E. M., Mukundan, R., Hoang, L., Moges, M., & Owens, E. M. (2019). Revisiting SWAT as a saturation-excess runoff model. *Water*, *11*(7), 1427. https://doi.org/10.3390/w11071427

Steenhuis, T. S., & Van der Molen, W. H. (1986). The Thornthwaite-Mather procedure as a simple engineering method to predict recharge. *Journal of Hydrology*, *84*, 221–229. https://doi.org/10.1029/1998WR900067

Tapley, B. D., Bettadpur, S., Ries, J. C., Thompson, P. F., & Watkins, M. M. (2004). GRACE measurements of mass variability in the Earth system. *Science*, *305*(5683), 503–505. https://doi.org/10.1126/science.1099192

Thornthwaite, C. W., & Mather, J. R. (1955). The water balance. *Publications in Climatology*, *8*(1).

Tilahun, S. A., Guzman, C. D., Zegeye, A. D., Dagnew, C. D., Collick, A. S., Yitaferu, B., & Steenhuis, T. S. (2015). Distributed discharge and sediment concentration predictions in the sub-humid Ethiopian highlands: The Debre Mawi watershed. *Hydrological Processes*, *29*, 1817–1828. https://doi.org/10.1002/hyp.10298

Tilahun, S. A., Mukundan, R., Demisse, B. A., Engda, T. A., Guzman, C. D., Tarakegn, B. C., et al. (2013). A saturation excess erosion model. *Transactions of the ASABE*, *56*(2), 681–695. https://doi.org/10.13031/2013.39257

Troch, P., van Loon, E., & Hilberts, A. (2002). Analytical solutions to a hillslope-storage kinematic wave equation for subsurface flow. *Advances in Water Resources*, *25*, 637–649. https://doi.org/10.1016/S0309-1708(02)00017-9

Troch, P. A., Berne, A., Bogaart, P., Harman, C., Hilberts, A. G. J., Lyon, S. W., et al. (2013). The importance of hydraulic groundwater theory in catchment hydrology: The legacy of Wilfried Brutsaert and Jean-Yves Parlange. *Water Resources Research*, *49*, 5099–5116. https://doi.org/10.1002/wrcr.20407

Troch, P. A., Paniconi, C., & van Loon, E. E. (2003). Hillslope-storage Boussinesq model for subsurface flow and variable source areas along complex hillslopes: 1. Formulation and characteristic response. *Water Resources Research*, *39*(11), 1316. https://doi.org/10.1029/2002WR001728

Van de Giesen, N., Steenhuis, T. S., & Parlange, J.-Y. (2005). Short- and long-time behavior of aquifer drainage after slow and sudden recharge according to the linearized Laplace equation. *Advances in Water Resources*, *28*, 1122–1132. https://doi.org/10.1016/j.advwatres.2004.12.002

Walker, G. R., Gilfedder, M., Dawes, W. R., & Rassam, D. W. (2015). Predicting aquifer response time for application in catchment modeling. *Groundwater*, *53*(3), 475–484. https://doi.org/10.1111/gwat.12219

Wilson, G. V., Nieber, J. L., Fox, G. A., Dabney, S. M., Ursic, M., & Rigby, J. R. (2017). Hydrologic connectivity and threshold behavior of hillslopes with fragipans and soil pipe networks. *Hydrological Processes*, *31*(13), 2477–2496. https://doi.org/10.1002/hyp.11212

Zegeye, A. D., Steenhuis, T. S., Blake, R. W., Kidnap, S., Collick, A. S., & Dadgari, F. (2010). Assessment of soil erosion processes and farmer perception of land conservation in Debre Mawi watershed near Lake Tana, Ethiopia. *Ecohydrology and Hydrobiology*, *10*(2–4), 297–306. https://doi.org/10.2478/v10104011-0013-8